Cover

基于离子阱的量子信息系统的控制系统开发

张君华　　物理

导师：金奇奂副教授

摘要

近几年，经典计算机的发展在物理实现上已经接近极限，经典的图灵机模型也始终无法有效解决 NP 问题。量子计算机作为一个新的研究领域，已经受到越来越多的重视。在量子计算机的物理实现领域，离子阱系统是最有前景的方向之一。离子阱实验的控制系统必须具有高速的响应和灵活的可编程性。本文首先给出一个关于量子计算和离子阱系统的基本背景，而后介绍了我们实验室的基于镱-171 离子的实验系统，最后提出一个基于计算机的全自动实验控制系统，并对系统的结构和其核心器件——脉冲序列发生器的设计进行深入的讨论。

关键词：量子信息，离子阱，控制系统

Developing a Control System for Quantum Information Processing with Trapped Ions

Zhang Junhua Physics

Directed by A.P. Kihwan Kim

Abstract

In recent years, classical computers have seen their boundaries, both physical and theoretical. Quantum computer, as a new research field, has been more and more widely explored. The trapped-ion system is a promising candidate for the physical implementation of quantum computer. An ultrafast control system with high programmability is required for the experiments of trapped-ion system. In this thesis, a simple background of quantum computation and trapped-ion system is first provided, followed by an introduction of our experiment system with $^{171}Yb^{+}$ ion. And finally, a computer-based automated control system is proposed, the core of which, the pulse sequencer, is also discussed in detail.

Keywords: Quantum Information, Trapped-Ion, Control System

Contents

I. Introduction

1. Quantum Computation

From 1925, the first field-effect transistor was invented, the density of transistors in IC chips, as well as the computational power of electronic devices, has been improving rapidly. According to the Moore's Law, this density doubles approximately every two years. However, such trend cannot be sustained indefinitely. As transistors become smaller, quantum mechanics starts to take effect, thus preventing a circuit from functioning classically. And it is shown that theoretically classical circuits are not likely to solve certain kind of problems efficiently, such as factorization. These problems are classified as NP problems in computability theory. Algorithms of polynomial complexity on classical Turing machine for them are unknown up to now.

So, what's the way out? Quantum computer might be the answer.

The concept of quantum computation was first introduced by Richard Feynman in 1982 [1] [2]. The basic unit of data for a quantum computer is qubit, named after its classical counterpart. A qubit can take the state of 0, 1, or their superposition state:

$$|\varphi\rangle = \alpha|0\rangle + \beta|1\rangle, \qquad |\alpha|^2 + |\beta|^2 = 1, \qquad \alpha, \beta \in \mathbb{C}$$

The state of a quantum memory which consists of N qubits is the direct product of the N single-qubit states:

$$|\Phi\rangle = \bigotimes_{i=1}^{N} |\varphi_i\rangle$$

Hence it has a degree of freedom of 2^N, which is much larger than that of a classical memory of same width.

Resembling classical logic gates, quantum gates are unitary operators in the Hilbert space of quantum memories with certain width:

$$|\Phi'\rangle = \widehat{U}|\Phi\rangle$$

From the linearity of quantum mechanics, it is easy to derive that:

$$\hat{U}(\alpha|\Phi_1\rangle + \beta|\Phi_2\rangle) = \alpha\hat{U}|\Phi_1\rangle + \beta\hat{U}|\Phi_2\rangle = \alpha|\Phi_1'\rangle + \beta|\Phi_2'\rangle$$

In other words, given a superposition of some states, the superposition of each result with same coefficient is generated. This property can be intuitively taken as "quantum parallelism". But, due to the state collapse after measurement, it is not possible to get all the results simultaneously, each time only one result can be revealed. However, since quantum mechanics deals with probability amplitude rather than probability itself, the coherence of quantum states can be utilized to maximize the coefficient of a chosen result, making it more probable to appear when the state is measured.

With the quantum parallelism and the ability to choose from the results, it is easy to imagine that quantum computer can perform exponentially as many tasks at the same time and show the required result. Shor's algorithm [3] is an ingenious example of utilizing these two properties, which is able to factorize an integer of n digits in polynomial time of n.

Apart from the quantum computation mentioned above, quantum mechanics has many other applications in the evolution of informatics, such as quantum simulation [4] [5], the main idea of which is to simulate the Hamiltonian of a physical system with a simpler, controllable quantum system and then explore the dynamics; quantum secure communication [6], which takes advantage of the quantum teleportation effect and no-cloning property of unknown quantum states to avoid eavesdropping during communication; and genuine random source, which simply utilizes the random nature of quantum mechanics.

It is quite promising that quantum mechanics will be the leading force of the next information revolution and change the very essence of data processing.

2. Physical Implementations of Quantum Computer

Nowadays there are many different ways on implementing a quantum computer. However, for any possible approach, some general criteria [7] shall be fulfilled. These criteria are called the DiVincenzo criteria, named after their proposer, David P. DiVincenzo in IBM. The criteria are as follows:

A scalable physical system with well-characterized qubits: The degrees of freedom required to hold data and perform computation shall be available as dimensions of the Hilbert space of a quantum system. And the dimension of the Hilbert space shall be definite while with the ability to scale up.

The ability to initialize the state of the qubits to a simple fiducial state: The qubits of the system shall be able to be initialized to certain states from any other possible states, as a start point of computation, with high precision and possibility.

Long decoherence times, much longer than the gate operation time: The system shall be well isolated from its environment, preventing its qubits from coupling to the surroundings, losing the coupling with each other. Since the ideal case is not possible for real systems, at least the decoherence time, that is, the time before a prepared state evolves out of a certain error tolerance, shall be long enough to carry out several gate operations.

A universal set of quantum gates: It shall be able to introduce some quantum gate operations, so that any other quantum gates can be realized with combinations of such gate operations.

A qubit-specific measurement capability: The qubits of the system shall have a strong interaction with the measurement apparatus, so that they are bound to be projected to a certain eigenstate of the observable when measured.

The ability to interconvert stationary and flying qubits: It shall be possible to enable communication between different kinds of system, or more specific, to enable the entanglement between an easy-to-hold qubit, such as an ion, and an easy-to-send qubit, such as a photon.

The ability to faithfully transmit flying qubits between specified locations: This is the direct follow-up of the previous criterion. The entangled easy-to-send qubit shall be possible to be precisely transmitted.

Here the first 5 criteria are for quantum computers, while the last 2 criteria are for quantum networks. At least the first 5 criteria are required for a functional prototype of quantum computer.

The main directions of approaching up to now and their brief introduction are listed below:

Photons [8]**:** In this regime, qubits are mainly realized as the polarization state of a photon, although the states of time and location are also available. The strong point is that photons do not possess strong interactions with the environment, hence the decoherence time is relatively long. While the drawback is that it is also difficult to introduce interactions between multiple photons, which are essential for multi-qubit control.

Nuclear Magnetic Resonance (NMR) [9]**:** The states of nuclear spin are used to encode qubits, which can be identified through the Larmor frequency if immersed in a strong magnetic field. Qubit manipulations in this kind of system are realized with resonant radio-frequency (RF) pulses of various durations. However, the major hurdle is the initialization and detection of qubits. No sufficient technique has been found up to now.

Quantum dots and dopants [10]**:** Quantum dots can be regarded as some kind of “artificial atoms”. They are small semiconductor nanostructure on the surface or impurities inside the solid material, which capable of trapping electrons or holes into a localized potential with discrete energy level, resembling atomic nuclei. In this system, it is easy to control one qubit, but since the range of interactions between quantum dots is extremely short and the quantum dots are immobile, to couple two arbitrary multiple quantum dots is a challenge.

Superconducting Circuits [11]**:** In superconductors at low temperature,

electrons bind into Cooper pairs that condense into a state with zero-resistance current and a well-defined phase. The quantized charge, flux and phase can all be used to encode qubits, of which the manipulation can be realized by changing macroscopically defined parameters like inductance and capacitance. This kind of devices resembles classical integrated circuits and can be easily fabricated using existing technologies. However, the superconducting qubit suffers a rapid decoherence due to the macroscopic scale of the system.

Neutral Atoms [12]**:** Crossed laser beams in free space form an optical lattice, which can be used to trap neutral atoms. The energy levels of the atoms in the potential well can be used as qubits. Typically an optical lattice is loaded with $10^3 - 10^6$ identical atoms, but addressing an individual atom still remains as a problem.

Trapped Ions: This is the main topic of this thesis. A detailed discussion is in the next section, explaining the basic scheme and how the trapped-ion system meets the requirements of the DiVincenzo criteria.

3. Trapped-Ion System

According to Maxwell's equations electrostatic field in free space with no charge satisfies:

$$\nabla \cdot \boldsymbol{E} = -\nabla^2 \varphi = 0$$

So there is no local minimum or maximum of the electric potential, thus unable to hold charged particles. However, for a rotating RF field, it forms a parabolic pseudo-potential if averaged over one period. If the frequency is high enough, this pseudo-potential is capable of holding particles of very small mass like atomic ions. If such kind of RF field is applied parallel to xy-plane, with a weak confinement along the z-axis, it is possible to trap multiple ions in one line with equal space between two adjacent ones. With the scheme mentioned above, an ion trap system can hold many ions with stable internal energy levels encoding qubits. This feature

satisfies the first criterion. However, in this way the number of ions cannot be increased by order of magnitudes. So the scalability of trapped-ion system also has its bottlenecks.

As to the second criterion, the initial state can be prepared with extremely high fidelity by optical pumping [13]. Ions in any energy levels other than intended are excited with laser, and then randomly decay into one of a series of energy levels including the intended one. After several rounds of excitation and decay, the ions will eventually populate the intended energy level.

Typically the ions are trapped in ultra-high vacuum (UHV) without any direct contact to the environment. So the decoherence time can be as long as several seconds, which is extremely long compared to the average gate operation time of microseconds, thus fulfilling the third criterion.

For the fourth one, it has been theoretically proved that with the combination of a set of one-qubit gates and two-qubit gates any possible quantum gates can be approximated. One-qubit gate in trapped-ion system can easily be implemented utilizing magnetic dipole transitions or electric quadrupole transitions. While two-qubit gates are realized through laser-induced coupling between spin of ions and phonons of collective harmonic modes [14].

While for the fifth criterion, the states of ions can be efficiently measured through the use of state-dependent optical fluorescence detection. The spectrum of the detection laser covers only the energy gap of two specific energy levels. If the ion is projected into one of the two states when measured, it will continuously be excited by the laser and emit photons, which can be collected by a photomultiplier tube (PMT) or a CCD camera. Otherwise, the ion just remains dark.

And finally for the last 2 criteria, ions and photons each make perfect stationary and flying qubits respectively, and the method to make them entangled has been proposed [15] [16]. This is another possible direction to scale up the capability of trapped-ion system.

In general, trapped-ion system meets all the DiVincenzo criteria to a great extent, and can be implemented with existing techniques. Compared with other types of approaches, it is most promisingly to provide a functional prototype of quantum computer in current state of technology.

II. Trapped-Ion System with $^{171}Yb^{+}$

1. General View

Our experimental trapped-ion system can be divided into several subsystems with different functions, as shown in Fig. 1.

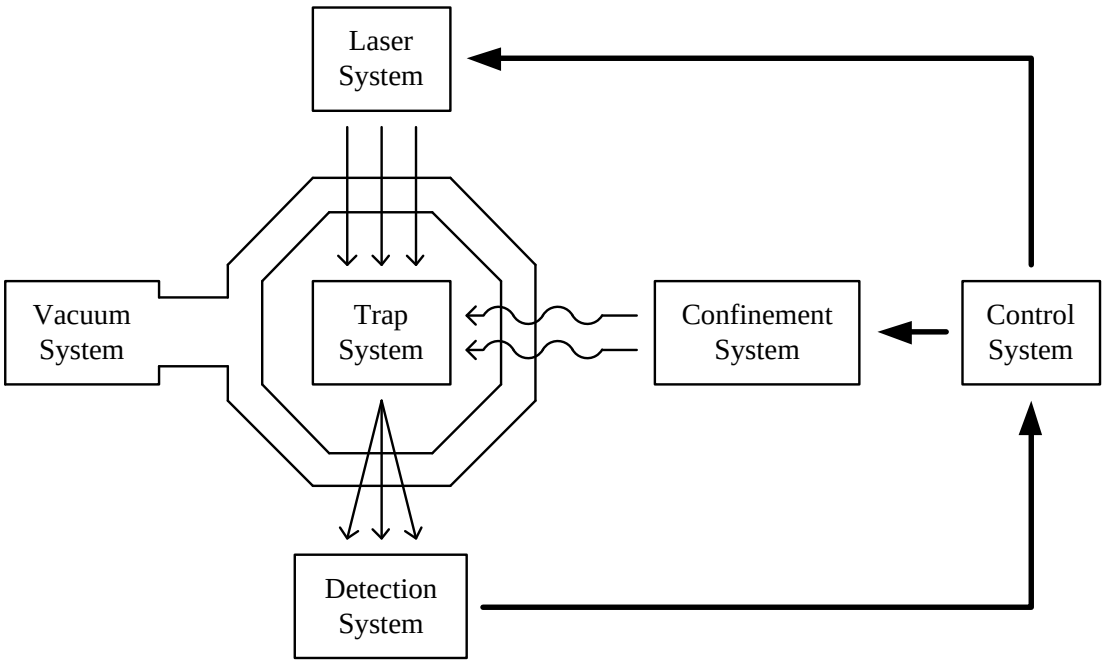

Fig. 1 | divisions of our experimental system

The vacuum system is used to provide an UHV condition for the ion trap to reduce the background collision rate, thus ensuring a relatively long lifetime of the ions.

The laser system is made up of lasers, cavities, electro-optic modulators and acousto-optic modulators. Its goal is to generate frequency-stabilized laser beams for Doppler cooling, optical pumping, state detection and coherent gate operation, etc.

The detection system, including a PMT and a CCD camera, is to detect the fluorescence of the ions. The CCD camera images the ions, while the PMT counts the actual number of the photons emitted from the ions.

And it comes to the kernel of the experiment system, the trap system. It consists of a 4-rod ion trap and 4 atomic ovens each with different fillings. Atoms are shot toward the trap when the ovens are heated up, then ionized by the laser beam at the center of the trap, and finally trapped by the confinement field generated by the confinement system.

As shown in the figure, the laser system, the confinement system and the detection system are all connected to the control system. It is responsible for precise manipulation of frequency and duration of the laser pulses, amplitude control of the confinement signals, and data acquisition and processing.

Detailed discussion for the vacuum, the trap system, the laser system and the detection system will be found in the following sections, while that for the control system is left for the next chapter.

2. Vacuum System

In order to maintain a long lifetime as well as a long decoherence time of the ions, background collisions, that is, collisions between the ions and the gas molecules, should be suppressed. That is why UHV condition is required for trapped-ion system. For properly loading one ion, the pressure should be as low as 10^{-10} torr. However, for experiments on the ion crystal which consists of multiple ions, a vacuum level of 10^{-13} torr is required.

Compared with normal vacuum condition, the underlying nature of UHV is quite different, and the efficiency of the pumps on pumping out different kinds of gas also matters a lot. So more pump stages and different techniques are needed to reach this level of vacuum. The layout of our vacuum system is in Fig. 2.

In the UHV region, the dominant factor of pressure increase is outgassing of the

vacuum components and evaporating of the water layer on the surface. So a furnace was utilized to heat the vacuum system to 200℃ for 1 week to quicken the outgassing and completely vaporize the water layer. When the baking was finished, the bakeable valve (H) was sealed before the temperature decrease to cut off the inner system from the outer one. The furnace was also used to perform air bake on vacuum components of the inner system before assembling to generate a chromium oxide coating. This coating is able to prevent the material of vacuum components from absorbing gases in the air, thus decreasing the amount of out gassing.

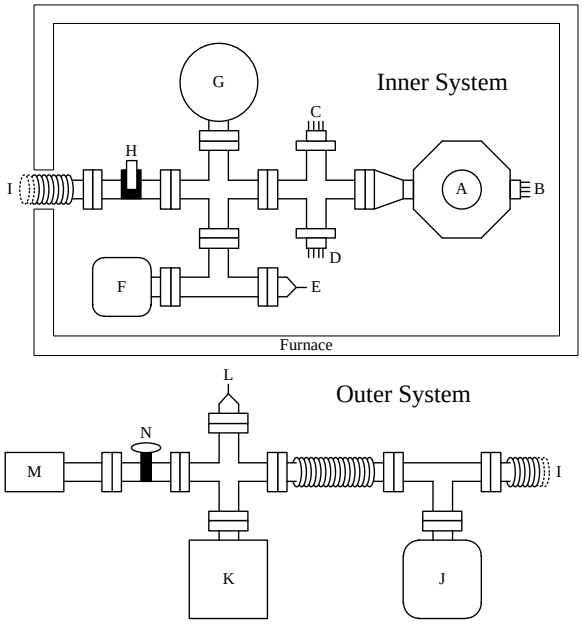

A octagon vacuum chamber for the trap system
B feedthrough for RF confinement voltage
C feedthrough for DC confinement voltage
D feedthrough for atomic ovens
E ion gauge
F small ion pump
G Ti sublimation pump
H bakeable valve
I bellows connecting the two systems
J big ion pump
K turbomolecular / mechanical pump assembly
L ion gauge
M residual gas analyzer (RGA)
N isolation valve for the RGA

Fig. 2 | design of the vacuum system

Fig. 3 | finished vacuum system

As shown in the figure, there are mainly 4 pump stages in our system. First, the turbomolecular pump and mechanical pump assembly (K), also with the big ion pump (J), lowered the pressure around the connection bellow (I) to 6.6×10^{-9} torr. After sealing the bakeable valve (H), the small ion pump was brought online to do further pumping. And finally, when the system was at room temperature, the Ti

sublimation pump was turn on to take out the hydrogen, which is the dominant ingredient in UHV environment. After all the pump stages, the pressure of the system, measured by the ion gauge (E), was as low as 10^{-11} torr. Then the bellow (I) and the bakeable valve (H) were disconnected, and the system was ready for the experiments (Fig. 3).

3. Trap System

In our system, we chose the classical 4-rod design of linear Paul trap [17] (Fig. 4), which was invented by Wolfgang Paul in 1953. 4 cylindrical electrodes with 2 of which connected to RF signal provide radial confinement, while 2 needle electrodes connected to DC voltage provide axial confinement. Sometimes the ions may be shifted from the center line of the trap by background electric field, so that a small oscillation of the ions will be excited by the RF field, which is called "micromotion". In order to prevent such effect, 2 extra cylindrical electrodes are added outside the trap to compensate the background electric field. The voltage of each micromotion compensation electrode as well as axial confinement electrode can be individually controlled through the control system.

Around the trap, 4 atomic ovens each filled with natural Yb, ^{171}Yb, natural Ba and ^{137}Ba are mounted as atom sources. When a DC current of typically 2A is applied to the stainless steel tube, the filling is heated up, then a beam of several thousand atoms is emitted from the oven to the trap. The main body of the oven is as shown in Fig. 5. When finally assembled, the vacuum chamber is like Fig. 6.

4. Laser System

Almost all the operations of ions are done by lasers addressing the ion's various energy gaps, so a highly stable laser system is important for the experiment. Currently we use $^{171}Yb^{+}$ ions (Fig. 7) in the experiments. At least the following operations are required:

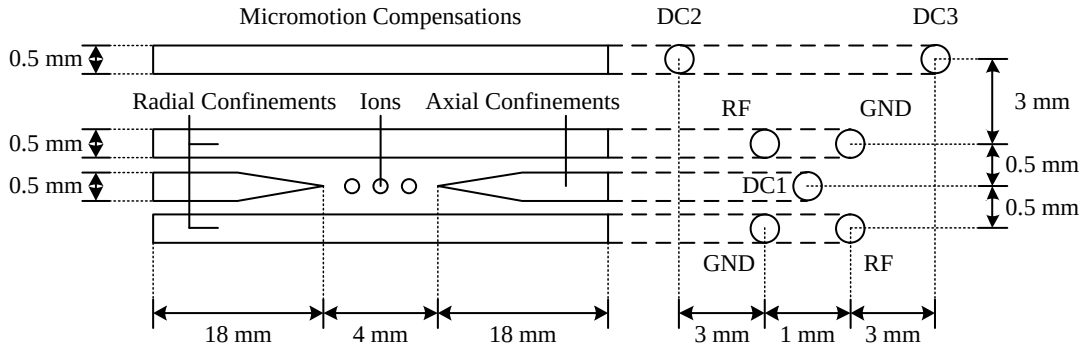

Fig. 4a | design of the trap

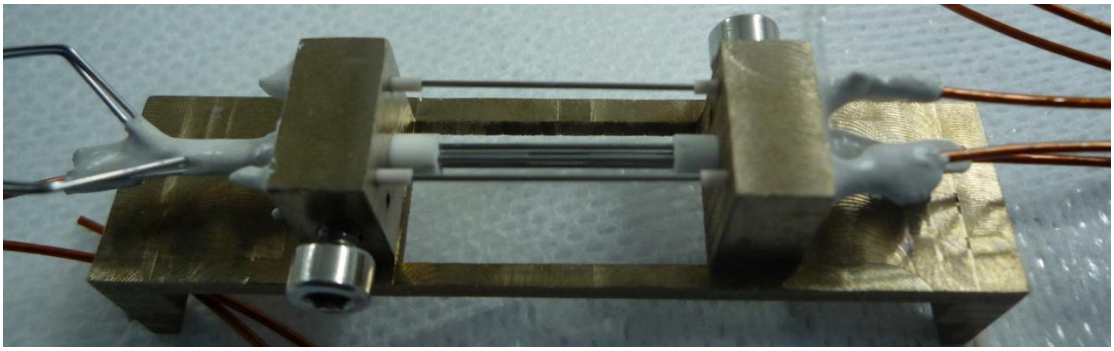

Fig. 4b | finished trap on its holder

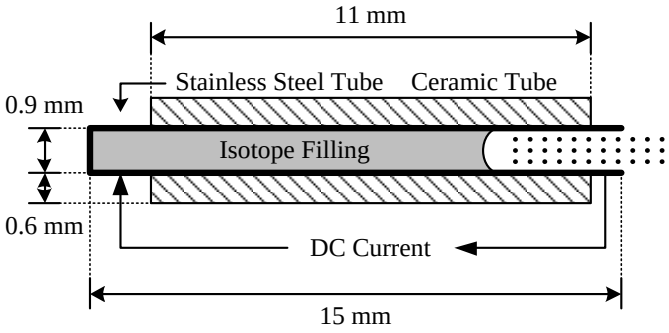

Fig. 5a | design of the oven

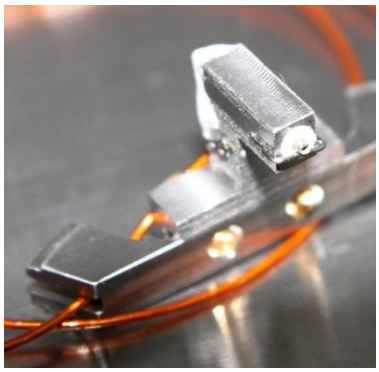

Fig. 5b | finished oven

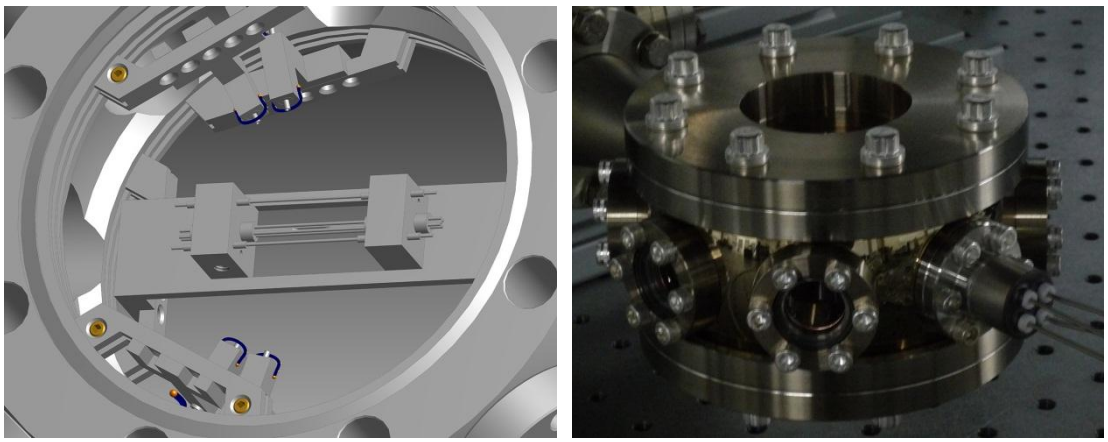

Fig. 6 | inside and outside view of the vacuum chamber

Ionization: The ^{171}Yb atoms should first be excited from $^{1}S_0$ to $^{1}P_1$ by a 399nm laser beam, and then ionized by a 370nm laser beam.

Doppler cooling: A modulated 370nm laser beam covering the hyperfine levels of $^{171}Yb^{+}$ ions' $^{2}S_{1/2}$ and $^{2}P_{1/2}$ states with 2GHz red detuning is required to decrease the momentum of the ions.

Optical pumping: A modulated 370nm laser beam covering all the hyperfine levels of $^{2}P_{1/2}$ state and state $^{2}S_{1/2}$, F=1 is required to initialized the ions to state $^{2}S_{1/2}$, F=0.

State detection: A 370nm laser beam covering only the energy gap of $^{2}P_{1/2}$, F=0 and $^{2}S_{1/2}$, F=1 is required to detect whether the ions are at state $^{2}S_{1/2}$, F=1.

Besides, laser beams of 935nm and 638nm are also necessary to bring the ions of metastable states $^{2}D_{3/2}$ and $^{2}F_{7/2}$ back to state $^{2}S_{1/2}$ respectively.

So, we have 4 different sets of laser in our system, with EOMs adding frequency sidebands and AOMs serving as optical switch, controlling the duration of laser beams (Fig. 8).

5. Detection System

The detection system is an essential part of the experiment system. It is responsible for imaging the ions and performing state detection. So its detection efficiency is vital to the fidelity of state preparation and quantum gate operation. The detection efficiency is mainly determined by two factors, the photon collection efficiency and the contrast between ions' fluorescence and background scattering.

Since the direction of the spontaneous emission of an ion is completely random, the easiest way to increase the photon collection efficiency is to maximize the solid angle of the detection lens to the ion. In our system, a microscopic objective lens with a short focal length and a large numerical aperture is used as the first stage of detection. As shown in Fig. 9, this objective lens images the ion at the center of an iris, then a group of magnifying lenses casts the image to the sensitive surface of

either the CCD camera or the PMT, switchable by a flipping mirror (Fig. 10b). From the numbers in the figure, it is easy to calculate that the detection efficiency determined by the solid angle of the objective lens is 0.77%.

As to the contrast, multiple methods are introduced to decrease the background level. Firstly, a 370nm narrow-band reflecting mirror and two filters of same wavelength are used to filter out photons of other wavelength. Secondly, an iris is placed on the image plane of the objective lens. When using PMT, it is adjusted to let only the image of the ion pass through, thus significantly reducing the background count. And finally, all the optical components are enclosed and fixed with lens tubes to ensure light-tightness. The first part of the lens tube assembly is mounted to a transition stage (Fig. 10a), which provides a firm support as well as a precise control of the image system, while the second part is directly fixed on the optical table to reduce the vibration.

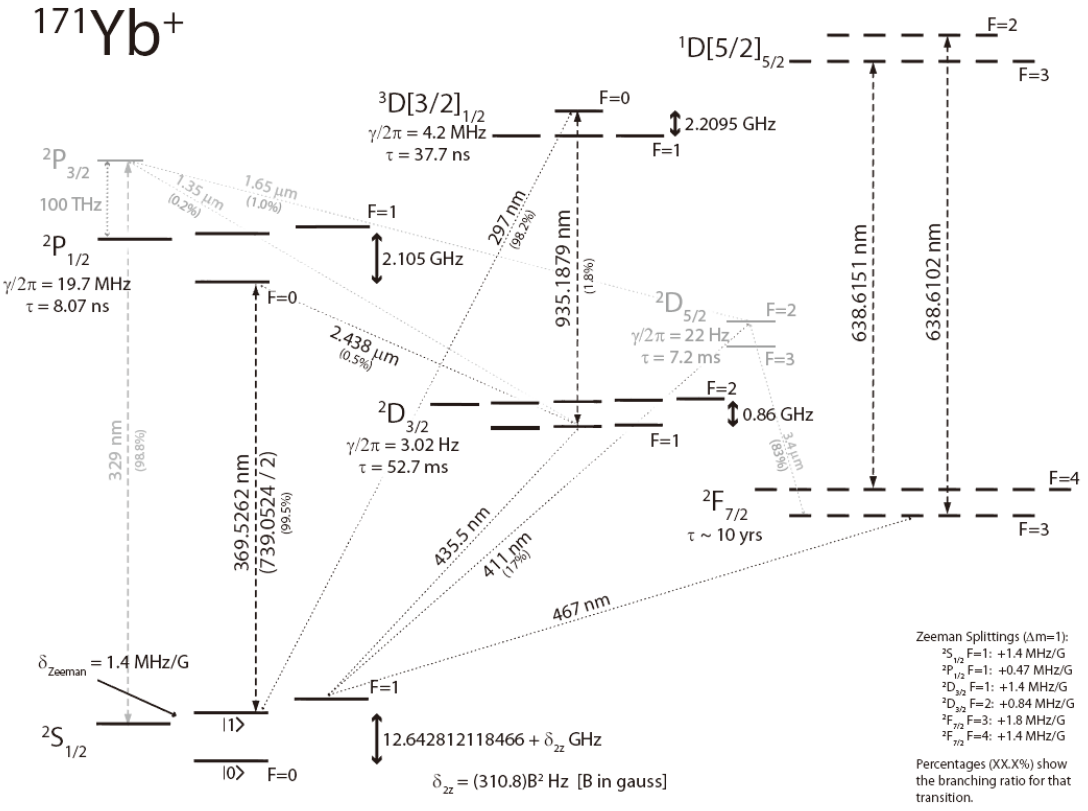

Fig. 7 | energy levels of $^{171}Yb^{+}$ ion

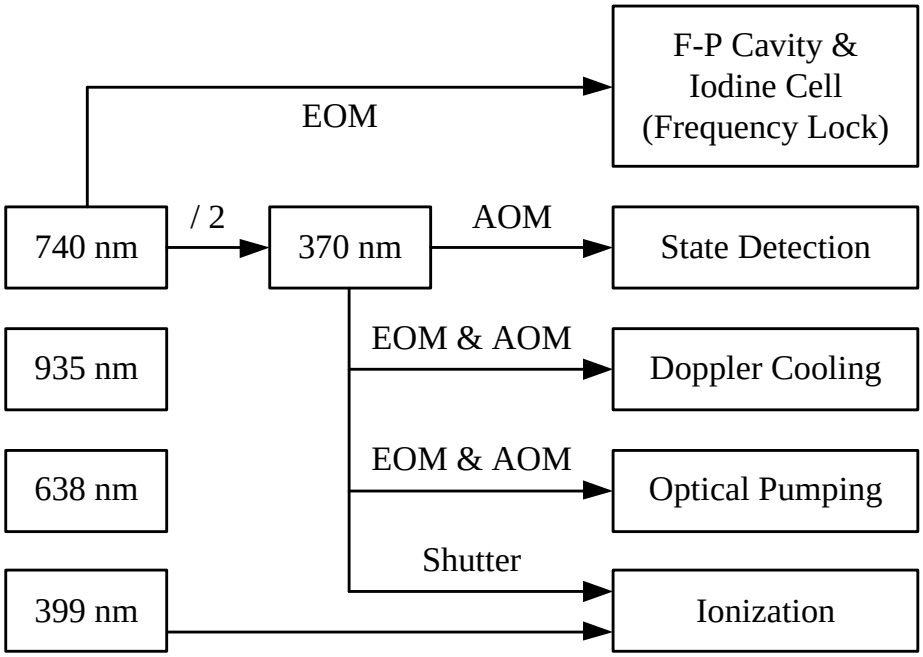

Fig. 8 | scheme of the laser system

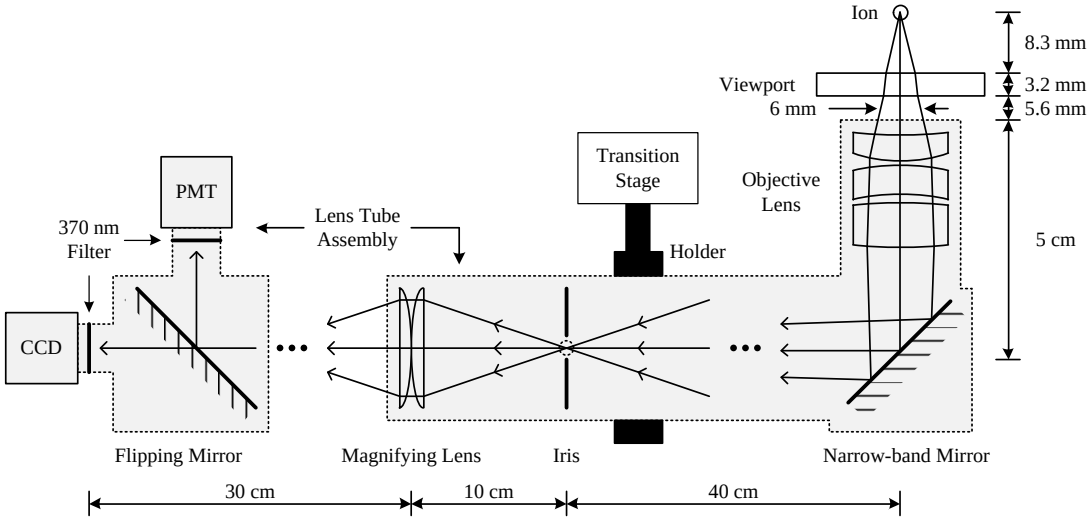

Fig. 9 | design of the detection system

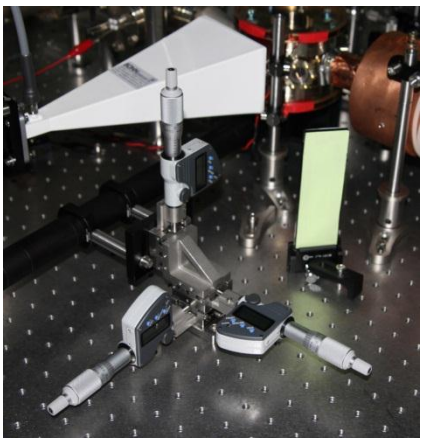

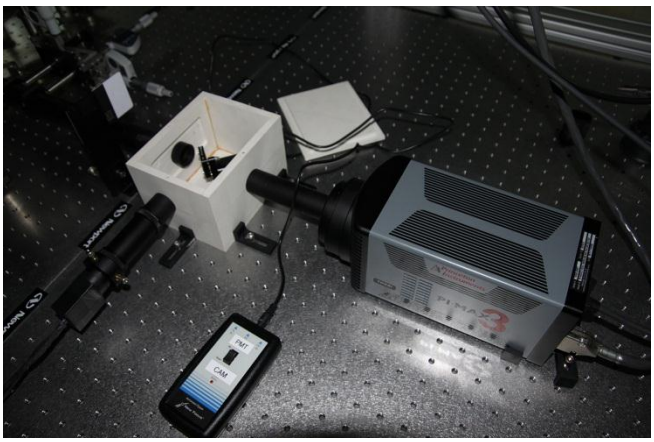

Fig. 10a | transition stage **Fig. 10b | CCD, PMT and flipping mirror**

Fig. 11 is a typical image of ions cropped from a frame of the CCD camera. The bright spots are the ions. Note that our detection system cannot actually image the ions, what are seen in the figure are in fact the Airy disks of the ions due to the diffraction limit of the objective lens. Because the light-sensitive part of the camera is a 1024×1024 CCD array of 1cm×1cm in size, the distance between the two adjacent spots is 2.597mm. Substituting the numbers into the formula of paraxial imaging, we have the actual distance of the two ions:

$$2.597\text{mm} \times \frac{10\text{cm}}{30\text{cm}} \times \frac{17.1\text{mm}}{450\text{mm}} = 32.9\mu\text{m}$$

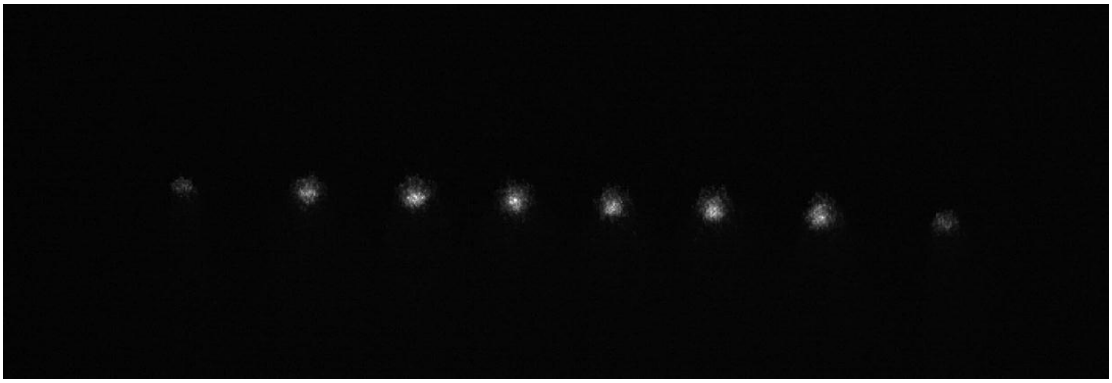

Fig. 11 | typical image of the ions

III. Control System

1. Motivation and Performance Requirements

For a successful experiment, the control of the apparatus is critical. A good control system can significantly reduce the overall time and increase the precision. Our experiments involve microsecond level optical switching, programmable frequency sweeping and large times of repetition of one experiment. All these requirements call for a computer-based automated control system.

More exactly, there are two kinds of operations involved:

Signal switching: Signals applied to the AOMs, EOMs and some other devices

should be sequentially enabled or disabled at microsecond level with precise timing. And the sequence and durations should be programmable.

Parameter sweeping: One experiment is carried out repetitively with one parameter linearly changing to obtain the relationship between the outcome and the parameter. Typically the number of repetition is at 10^4 level.

For example, a simple experiment to test the relationship between the duration of optical pumping and the fidelity of state preparation is like this:

a. Doppler cooling beam on, for 3000μs.
b. Doppler cooling beam off, optical pumping beam on, for Dμs.
c. Optical pumping beam off, detection beam and counter on, for 800μs.
d. All off, for 30μs.
e. Repeat step a-d for 100 times with same parameter D to get the fidelity.
f. Sweep the value of D, from 0.1 to 10 with step length 0.1 to get the relationship of the fidelity and the duration of optical pumping.

It is obvious that the programmability calls for a computer to be the control terminal, but the timing requirement is beyond the capability of computer programs.

2. Structure of the Control System

Because of the performance requirements, we use a pulse sequencer (Fig. 13a) made from a general-purpose FPGA board of Altera CycloneII EP2C5T144C6 to control the time-critical devices such as AOMs and EOMs, while the main control panels are Visual Instruments (VIs) of LabVIEW in the computer (Fig. 13b). The structure of our control system is in Fig. 12.

The most of the parameters of the devices such as the frequency and wave pattern of the function generators are set directly by the computer VI. While the on/off operation sequence of time-critical devices is sent to the pulse sequencer, which is capable of reproducing the sequence in the form of TTL outputs to control the pulse switches and hence the optical modulators. A detailed technical discussion

of the pulse sequencer will be in the next section.

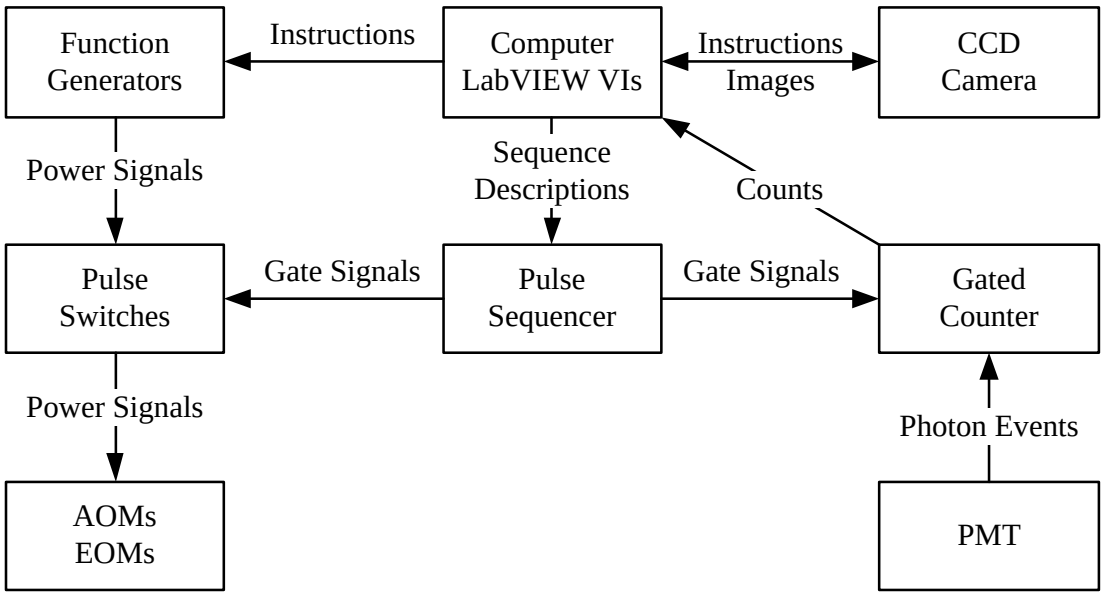

Fig. 12 | structure of the control system

Fig. 13a | pulse sequencer

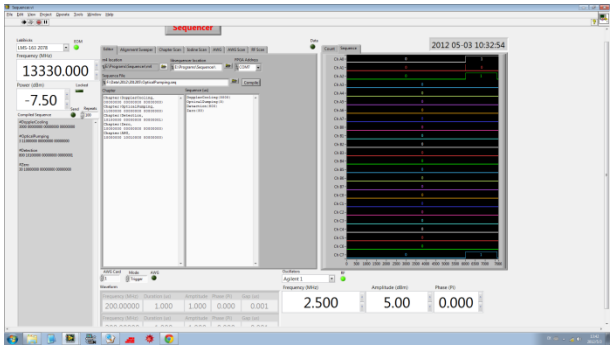

Fig. 13b | front panel of the pulse sequencer

3. Pulse Sequencer

In order to maximize the circuit performance, only the most time-critical task, in this case the timing of the sequence, are performed by the hardware. A sequence is descripted as a series of segments, each of which is a continuous period of time that no output port of the pulse sequencer changes its electrical level. Each segment has two fields, the duration of current segment and the output levels. When a segment is over, the next segment is loaded, refreshing the output level and the state of the timer, and then the timer continues to count down.

Our pulse sequencer is able to manage 24 independent output ports, with a range of durations from 2ns to 4,194,304ns and a maximum of 2560 segments in length. The diagram of the FPGA program is in Fig. 14, and the description of the signals and the modules is as follows:

Signal Name	Width	Description
USB Input	1 bit	This is the binary flow of instructions sent by the computer via USB-simulated virtual serial port.
Sequence Packet	45 bit	Each “Sequence Packet” defines one sequence segment, containing its duration and output levels.
Repetition	12 bit	This is the number of repetition that the sequence should be executed.
Received Flag	1 bit	This is a 1-cycle flag signal, indicating that the last packet of a sequence is received.
Finish Flag	1 bit	This is a 1-cycle flag signal, indicating that a full repetition of current sequence is finished.
Init Flag	1 bit	This is a multi-cycle flag signal, which directs module “FIFO Array” to perform initialization.
Disable Flag	1 bit	This is a lasting flag signal to control module “Timer”. When it is high, module “Timer” is suspended.
Tick	1 bit	This is a 1-cycle flag signal, indicating that current segment is over.
Duration	21 bit	This is the duration of current segment, in number of clock cycles.
Level	24 bit	This is the output levels of current segment.

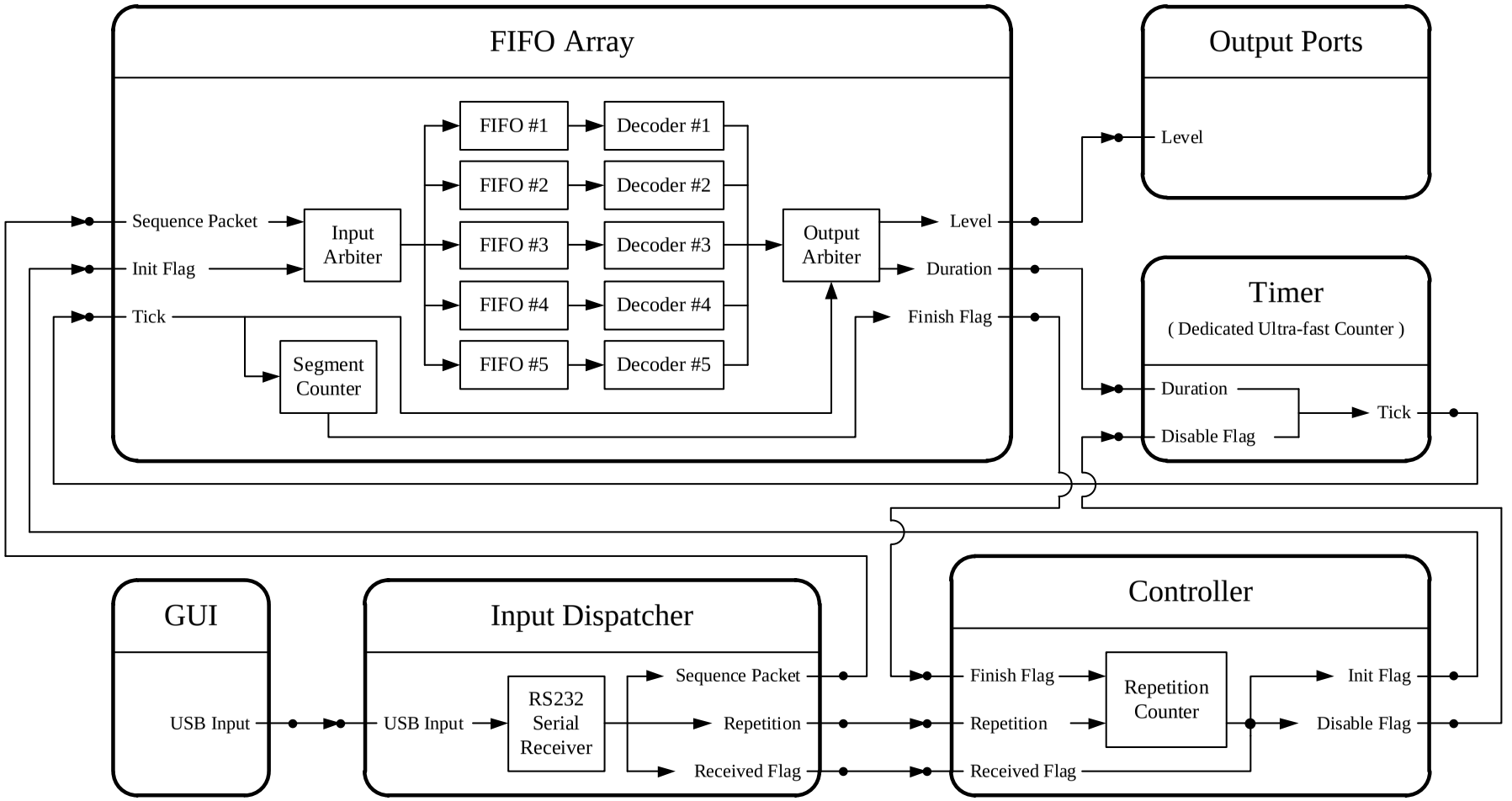

Fig. 14 | diagram of the pulse sequencer

Input Dispatcher: This module is to process and dispatch the incoming binary flow of instructions sent by the computer. Submodule “RS232 Serial Receiver” processes the incoming signal “USB Input”, and then submits the data in the form of packets. “Input Dispatcher” extracts signal “Repetition” from the first packet of current sequence and multiple “Sequence Packet” signals from following packets. Finally when the last packet is received, it asserts “Received Flag” signal.

Controller: The main task of this module is to control the state of the pulse sequencer. When signal “Received Flag” is asserted, indicating arrival of a new sequence, “Controller” generates “Init Flag” signal and then deasserts “Disable Flag” signal to enable module “Timer”. Signal “Finish Flag” triggers submodule “Repetition Counter”, which counts the repetition of the sequence. When the required times of repetition, defined by signal “Repetition”, are executed, it asserts signal “Disable Flag” to suspend module “Timer”.

FIFO Array: This module serves as a buffer of the sequence. A 5-channel parallel scheme is implemented to distribute the read-convert procedure of about 10ns into 5 clock cycles to achieve a minimal segment duration of 2ns. When a “Sequence Packet” signal is received, “FIFO Array” stores it in one of the 5 First-In-First-Out (FIFO) submodules. An “Input Arbiter” is used to address the 5 FIFOs one after another. It also clears the 5 FIFOs when signal “Init Flag” is high. When signal “Tick” is asserted, packets are read from the FIFOs one by one in the same order as input under the control of “Output Arbiter”. The data of signal “Level” is sent to refresh the output electrical levels of the output ports. And the data of “Duration” is transformed by Decoders to the form acceptable for “Timer”. Signal “Tick” also triggers “Segment Counter”, which counts the number of executed segments. When it equals the length of the sequence, it is reset to zero and signal “Finish Flag” is asserted.

Timer: This module is a dedicated ultrafast counter, which is capable of performing a +1 or -1 operation of arbitrary bit width in one clock cycle. If signal “Disable flag” is low, “Timer” continuously counts the clock cycles. When it meets the number defined by signal “Duration”, it asserts signal “Tick” and starts over again. Otherwise it is disabled.

IV. Conclusion

V. Reference

[1] R. Feynman, Simulating Physics with Computers, International Journal of Theoretical Physics, 1982, Vol. 21 (6-7): 467-488

[2] D. Deutsch and A. Ekert, Quantum Computation, Physics World, March 1998: 47-52

[3] P. W. Shor, Polynomial-Time Algorithms for Prime Factorization and Discrete Logarithms on a Quantum Computer, SIAM J. on Computing, 1997, Vol. 26: 1484-1509

[4] S. Lloyd, Universal Quantum Simulators, Science, 1996, Vol. 273: 1073-1078

[5] I. Buluta and F. Nori, Quantum Simulators, Science, 2009, Vol. 326: 108-111

[6] R. Hughes and J. Nordholt, Refining Quantum Cryptography, Science, 2011, Vol. 333: 1584-1586

[7] D. P. DiVincenzo, Topics in Quantum Computers, Mesoscopic Electron Transport, L. Kowenhoven, G. Schoen and L. Sohn (Vol.345, NATO ASI Series E, Kluwer, 1997), 657-679

[8] J. L. O'Brien, Optical Quantum Computing, Science, 2007, Vol. 318: 1567–1570

[9] N. A. Gershenfeld and I. L. Chuang, Bulk Spin Resonance Quantum Computation, Science, 1997, Vol. 275: 350–356

[10] B. E. Kane, A Silicon-based Nuclear Spin Quantum Computer, Nature, 1998, Vol. 393, 133–137

[11] Y. Nakamura, Yu. A. Pashkin and J. S. Tsai, Coherent Control of Macroscopic Quantum States in a Single-Cooper-pair Box, Nature, 1999, Vol. 398, 786–788

[12] O. Morsch and M. Oberthaler, Dynamics of Bose-Einstein Condensates in Optical Lattices, Rev. Mod. Phys. , 2006, Vol. 78: 179–215

[13] T. R. Carver, Optical Pumping, Science, 1963, Vol. 141: 599–608

[14] J. I. Cirac and P. Zoller, Quantum Computations with Cold Trapped Ions, Phys. Rev. Lett. , 1995, Vol. 74: 4091–4094

[15] D. L. Moehring, et al. , Entanglement of Single-atom Quantum Bits at a Distance, Nature, 2007, Vol. 449: 68-71

[16] L. Luo, et al. , Protocols and Techniques for a Scalable Atom-Photon Quantum Network, Fortschritte der Physik, 2009, Vol. 57: 1133-1152

[17] W. Paul and H. Steinwedel, Ein neues Massenspektrometer ohne Magnetfeld, Zeitschrift für Naturforschung A, 1953, Vol. 8: 448-450

VI. Acknowledgement